dination for both metal ions to streptonigrin.

Consider now the redox and catalytic properties of complex I. The addition of NADH to Pd-SN (I), which is EPR silent, in the absence of O_2 yields complex I'. The EPR spectrum of complex I' is characteristic of the presence of a free radical, indicating that the quinone group of streptonigrin has been reduced by NADH to semiquinone according to eqs 1a and 1b.

$$\underset{\text{I}}{\text{Pd-SN}} + \text{NADH} \rightarrow \text{Pd-SN}^{2-} + \text{NAD}^+ + \text{H}^+ \quad (1a)$$

$$\underset{\text{I}}{\text{Pd-SN}} + \text{Pd-SN}^{2-} \rightarrow 2\underset{\text{I}'}{\text{Pd-SN}^{\bullet -}} \quad (1b)$$

In the absence of oxygen, complex I', involving the semiquinone, is very stable. The addition of molecular oxygen to complex I' yields a new complex (I'') that we suggest to be a superoxo-Pd(II) complex.

$$\underset{\text{I}'}{\text{Pd-SN}^-} + \text{O}_2 \rightarrow \underset{\text{I}''}{\text{Pd-SN-O}_2^{\bullet -}} \quad (2)$$

Complex I'' is not stable and as time elapses decomposes to give complex I most likely according to eq 3. Equations 1-3 are

$$\underset{\text{I}''}{\text{Pd-SN-O}_2^-} \rightarrow \underset{\text{I}}{\text{Pd-SN}} + \tfrac{1}{2}\text{O}_2 + \tfrac{1}{2}\text{O}_2^{2-} \quad (3)$$

compatible with the observation that, in the system Pd-SN, NADH, O_2, 1 mol of NADH is reduced/mol of O_2 consumed: the combination of eqs 1-3 yields

$$\text{NADH} + \text{O}_2 \rightarrow \text{NAD}^+ + \text{H}^+ + \text{O}_2^{2-}$$

When the same experiment is performed in the presence of cyt c^{3+}, the first two steps of the reaction still occurred according to eqs 1 and 2. However, in the third step complex I'' reduces cyt c^{3+} according to

$$\underset{\text{I}''}{\text{Pd-SN-O}_2^{\bullet -}} + \text{cyt } c^{3+} \rightarrow \underset{\text{I}}{\text{Pd-SN}} + \text{cyt } c^{2+} + \text{O}_2 \quad (4)$$

Equations 1, 2, and 4 are compatible with the observation that in the system Pd-SN, NADH, cyt c^{3+} no oxygen is consumed overall and 2 mol of cyt c^{3+} is reduced when 1 mol of NADH is oxidized: the combination of eqs 1, 2, and 4 yields

$$\text{NADH} + 2\text{cyt } c^{3+} \rightarrow \text{NAD}^+ + 2\text{cyt } c^{2+} + \text{H}^+$$

These equations perfectly explain our data. Moreover, the reduction of cyt c^{3+} by Pd-SN-$O_2^{\bullet -}$ is in agreement with previous observations that reduction of cyt c^{3+} is not restricted to free $O_2^{\bullet -}$.[26] We must add that cyt c^{3+} is not reduced by complex I'. On the other hand, the observation that eqs 3 and 4 are not inhibited by superoxide dismutase is also in agreement with the fact that this enzyme is highly selective and is able to dismute free superoxide radical and not superoxide radical bound to the complex.

In this work we have shown that, in the absence of O_2, Pd-SN is able to react with NADH, while there is no reaction of NADH with free streptonigrin. In the absence of O_2, Pd-SN is able to catalyze the oxidation of NADH by O_2 whereas free streptonigrin is unable to do that in the absence of NADH dehydrogenase.

In conclusion, our data provide direct evidence that streptonigrin can form with metal ion complexes that are able to activate oxygen.

Acknowledgment. This work was supported by grants from the University Paris Nord, CNRS, and Institut Curie. We are indebted to the Laboratoire Rhône Poulenc and the NCI (Bethesda, MD) for supplying us with streptonigrin. We thank F. Lavelle (Rhône Poulenc Santé) for the inhibition cell growth assay and B. Maurin for technical assistance in the EPR measurements.

(26) Michelson, A. M. In *Superoxide and Superoxide Dismutase*; Michelson, A. M., McCord, J. M., Fridovich, I., Eds.; Academic Press: London, 1977; pp 77-106.

Contribution from the Biodynamics Institute, Choppin Hall, Louisiana State University, Baton Rouge, Louisiana 70803-1804

Mechanism of Catalase Activity in Aqueous Solutions of Dimanganese(III,IV) Ethylenediamine-*N*,*N*'-diacetate

James D. Rush* and Zofia Maskos

Received June 7, 1989

Manganous ions, ligated by ethylenediamine-*N*,*N*'-diacetate (edda = L) decompose hydrogen peroxide with a rate law $-d[H_2O_2]/dt = k_{17}[\text{Mn(edda)}][H_2O_2]$ where $k_{17} = 5.4\ M^{-1}\ s^{-1}$ at pH 7. The reduction of peroxide to water is initiated by the reaction of $Mn^{II}L$ with a dinuclear $Mn^{III,IV}L_2$. A subsequent fast reaction between the transient product of this reaction and hydrogen peroxide or *tert*-butyl hydroperoxide effectively oxidizes Mn(II) to Mn(IV) in a concerted step without formation of the hydroxyl radical. The green mixed-valence complex, which is probably a bis(μ-oxo)-bridged structure, is stable in neutral aqueous solution and exhibits a 16-line ESR signal in frozen solution. The basis of catalase activity is the autocatalytic formation of this complex when hydrogen peroxide is reduced by manganese(II) according to the overall reaction $Mn^{II}L + Mn^{III}L + H_2O_2 \xrightarrow{Mn^{III,IV}L_2} Mn^{III,IV}L_2$. The catalase cycle is independent of the formation of oxy radicals. Mononuclear Mn^{III}edda and Mn^{II}edda react with superoxide radicals, but the decomposition of peroxide is virtually independent of these reactions. In unbuffered solutions, with a moderate excess of hydrogen peroxide, an oscillation in the concentration of the dinuclear complex is detected.

Introduction

A multinuclear manganese unit is well-known to be central to the oxidation of water to O_2 during photosynthesis.[1] A less investigated biological use of multinuclear manganese is in the catalase of certain bacteria, that of *Lactobacillus* plantarum having been the most studied.[2] Many manganese complexes have been investigated for structural[3] as well as functional[4] similarities to these systems. The essential step in an efficient catalase must be the reduction of hydrogen peroxide without the formation of the OH radical, which attacks organic materials at near-diffusion-controlled rates. In general, mononuclear manganous com-

(1) (a) Dismukes, G. C. In *Manganese in Metabolism and Enzyme Function*; Schram, V. L., Wedler, F. C., Eds.; Academic: Orlando, FL, 1986; p 276. (b) Renger, G. *Angew. Chem., Int. Ed. Engl.* **1987**, *26*, 643 and references therein.

(2) (a) Kono, Y.; Fridovich, I. *J. Biol. Chem.* **1983**, *258*, 6015. (b) Beyer, W. F., Jr.; Fridovich, I. *Biochemistry* **1985**, *24*, 6460-6467. (c) Beyer, W. F., Jr.; Fridovich, I. In *Manganese in Metabolism and Enzyme Function*; Schramm, V. L., Wedler, F. C., Eds.; Academic: Orlando, FL, 1986; p 193.

(3) (a) Sheats, J. E.; Czernuszewicz, R. S.; Dismukes, G. C.; Rheingold, A. L.; Petrouleas, V.; Stubbe, J.; Armstrong, W. H.; Beer, R. H.; Lippard, S. J. *J. Am. Chem. Soc.* **1987**, *109*, 1435. (b) Cooper, S. R.; Dismukes, G. C.; Klein, M. P.; Calvin, M. *J. Am. Chem. Soc.* **1978**, *100*, 7249. (c) Mabad, B.; Tachuagues, J.-P.; Hwang, Y. T.; Hendricksen, D. N. *J. Am. Chem. Soc.* **1985**, *107*, 2802. (d) Weighardt, K.; Bossek, U.; Ventar, D.; Weiss, J. *J. Chem. Soc., Chem. Commun.* **1985**, 347. (e) Weighardt, K.; Bossek, U.; Zsolnai, L.; Huttner, J.; Blondin, G.; Girard, J.-J.; Babonneau, F. *J. Chem. Soc., Chem. Commun.* **1987**, 651.

(4) (a) Bodini, M. E.; Sawyer, D. T. *J. Am. Chem. Soc.* **1976**, *98*, 8366. (b) Awad, M. K.; Anderson, A. B. *J. Am. Chem. Soc.* **1989**, *111*, 802.

0020-1669/90/1329-0897$02.50/0

plexes are oxidized slowly, if at all, by H_2O_2, owing to the high reduction potentials of the manganic species[5] and the free energy of formation of the OH radical. It is unclear how polynuclear manganese-containing catalases exploit the favorable energetics for two-electron reduction of peroxide to water, $E°'(H_2O_2,2H^+/2H_2O) = 1.32$ V.[6]

We describe in this report the mechanism of the catalase activity exhibited by solutions of manganese(II) ethylenediamine-*N,N'*-diacetate (L = edda). The active catalytic species in solution is mixed-valence $Mn^{III,IV}L_2$, a complex that exhibits an ESR signal similar to that recently reported for the *Lactobacillus* active site[7] though differing in its optical spectrum,[2a] which has been compared with that for dinuclear manganese(III).[3a] The mechanism of peroxide reduction in the model system is a two-electron process that may have parallels in the action of *Lactobacillus* and other manganese-containing bacterial catalases.

The nature of the system that is described here admits many potential reactions and the participation of various oxidation states of manganese as well as oxygen. Some evidence of the potential complexity may be inferred from the fact that the concentration of the mixed-valence complex (probably a bis(μ-oxo)-bridged system) exhibits oscillations under certain conditions. Therefore, in addition to describing the catalase system, we have also conducted experiments to characterize as much as possible the species in solution and their likely roles in the overall mechanism. For instance, pulse radiolysis was used to elucidate processes in the catalase cycle that might involve superoxide radicals.

Experimental Section

Preparations. $[Mn^{III,IV}(edda)_2(O)_2]^-$(aq). Solutions of the dinuclear $Mn^{III,IV}$edda complex can be prepared by dissolving commercial manganic acetate or $Mn^{III,IV}(bpy)_4O_2(ClO_4)_3·2H_2O$ ($Mn^{III,IV}$bpy) in neutral solutions of the ligand or by oxidation of Mn^{II}edda with H_2O_2. Aqueous solutions of pH 6–7 are stable for several hours. The complex hydrolyzes and decomposes above pH 7.5. The ratio of ligand to metal in solution as 1:1 was determined by peroxide titration with excess ligand vs titrations with excess manganese(II). Evidence for the bis(μ-oxo) structure and oxidation state is described in the text. The solid complex was not isolated since concentration of these solutions leads to precipitation of crystalline manganese dioxide. An impure product in very low yield, which redissolved to give the green $Mn^{III,IV}$edda was precipitated from chilled (−10 °C), ethanolic solutions of the complex. Its infrared spectrum (KBr pellet) gave, in addition to ligand bands, a strong broad absorbance at 560 cm^{-1}.

Mn^{II}edda. The white Mn^{II}edda complex can be obtained by addition of an equivalent amount of a Mn(II) salt to a 0.5 M solution of the ligand. Then 1 M NaOH was added to effect dissolution at pH 6 and the complex precipitated out within a minute. Analysis for manganese by oxidation to permanganate gave the ligand to metal ratio as 1:1. The solution ESR spectrum of this species is a broad resonance (~500 G) at $g = 2.0$. The literature stability constant of Mn^{II}edda, log $[K(Mn^{2+} + edda^{2-})] = 7.05$,[8] was checked by standard titration methods.[9]

Methods. ESR spectra were taken on an IBM ER200D spectrometer at X-band frequencies (9.45 GHz) and microwave power of 2 mW. Samples were frozen with liquid N_2 after preparation, and most measurements were made at 130 K. One experiment was performed at 10 K on a Varian Century Series spectrometer at 9.26 GHz. Electrochemical measurements were made at ambient temperature with a Princeton Instruments voltammetric analyzer. Cyclic voltammetry was done in deaerated 5 mM solutions of $Mn^{III,IV}$edda containing 1–2 mM of stabilizing Mn^{II}edda and 0.1 M $NaClO_4$ as electrolyte. The solutions were buffered at pH 6.7 with HEPES buffer and excess edda. Static measurements of the overall (three-electron) reduction potential of the complex were made by progressive oxidation of a 0.01 M Mn^{II}edda solution with measured amounts of peroxide. This method was determined to give solutions of manganic ion to within about ±3–5% of the expected titer. Plots of log $([Mn(II)]^3/[Mn(III,IV)])$ vs emf were Nernstian with a slope of 2.95 from which the overall reduction potential was calculated.

In the determination of oscillations in potential of solutions during catalase activity, the available apparatus required that the electrode potential be fixed while oscillations in the current were recorded. To compensate for possible electrode effects, measurements were made in stirred and unstirred solutions, with both anodic and cathodic currents. Oxygen evolution was measured with a YSI Model 5350 oxygen-sensitive microelectrode and monitor.

Kinetic Measurements. Pulse-radiolysis experiments were carried out with the 2-MeV Van de Graaf accelerator at Brookhaven National Laboratory according to procedures described elsewhere.[10] Doses were computed with the KSCN dosimeter, assuming $G((SCN)_2^-) = 6.13$. As a result of radiolysis, the G values, or yields of radicals/molecular products formed per 100 eV of energy absorbed by water are[11]

$$H_2O \rightsquigarrow e_{aq}^- (2.65), H (0.65), OH (2.75), H_2O_2 (0.72), H (0.45)$$

Experiments in oxygenated formate solutions (0.01 M) converted the primary radicals to superoxide radicals. In the same solution, degassed with argon, the strongly reducing CO_2^- radical and the aquated electron remain after the pulse. The chemistry of these systems is described in standard texts.[12]

Ordinary kinetic experiments were run in a recording spectrophotometer or in a stopped-flow spectrometer (Kinetic Instruments) with data acquisition system from OLIS Inc. Kinetic simulations of spectrophotometer traces were performed with the program KINSIM. The formation of $Mn^{III,IV}$edda was usually monitored at 380 nm and checked elsewhere in the visible range. Of the reactions studied, experiments with added $NaClO_4$ indicated no ionic strength dependence, and this was not monitored further. A variety of buffer systems were used. Phosphate and cacodylate ions complex Mn^{III}edda. The amine buffers HEPES and MOPS were inert and used at pH ~7, but an excess of the edda ligand (0.01 M) was found most useful since it ensures full complexation of Mn(II) in solution. Hydrogen peroxide concentrations were determined by the absorbance of its complex with titanium(IV) in 2 M H_2SO_4 (ϵ(408 nm) = 740 M^{-1} cm^{-1})[13]

Materials. The complex $Mn^{III,IV}(bpy)_4O_2(ClO_4)_3·2H_2O$ was prepared and purified by a literature procedure.[14] Ethylenediammine-*N,N'*-diacetic acid, di-*tert*-butyl peroxide, nitro-blue tetrazolium (NBT) and manganic acetate were from Aldrich. Tetranitromethane (TNM) was obtained from K&K Laboratories and was prepared for use as described in ref 15. NBT and TNM react with superoxide radicals at rates of 5.9×10^4 and 2.0×10^9 M^{-1} s^{-1}, respectively.[16] For pulse-radiolysis studies, ultrapure (99.99%) $MnSO_4·4H_2O$ was used; otherwise, the perchlorate and chloride Mn(II) salts were used. Other common chemicals were of reagent grade. Water was purified by reverse osmosis and Millipore filtered.

Results

Characterization of the $Mn^{III,IV}$(edda) Complex in Solution. The green complex formed by action of peroxide in Mn^{II}edda is a mixed-valence species containing manganese and the ligand in 1:1 mole ratios. The stoichiometry for peroxide oxidation of a manganous solution ($[H_2O_2]/[Mn(II)] = 0.68$) is consistent with an average oxidation state of +3.5. Relatively little peroxide is lost due to its oxidation when Mn(II) is mainly in excess, as verified by oxygen electrode measurements (3–5% of peroxide is converted to O_2 during the titration of 6.5 mM Mn^{II}edda with 0.01 M H_2O_2). *tert*-Butyl hydroperoxide also is an efficient oxidant if a small amount of the manganic complex is initially added to the Mn^{II}edda solution.

The complex is also obtained by dissolving either manganic acetate or the $Mn^{III,IV}$bpy complex in a ligand solution at pH 6–7. The former method gives a slightly different absorption spectrum due to the presence of free Mn^{II}edda and a mononuclear Mn(III) complex (vide infra). The latter method is rapid and virtually quantitative. The absorption spectra of the complexes between pH 4 and pH 6.5 are shown in Figure 1.

Frozen solutions of the complex at pH 6–7 give a 16-line ESR signal of intensity (at 130 K) equal to that of the mixed-valence

(5) Yamaguchi, K. S.; Sawyer, D. T. *Isr. J. Chem.* **1985**, *25*, 164 and references therein.
(6) Koppenol, W. H.; Butler, J. *Adv. Free Radical Biol. Med.* **1985**, *1*, 91.
(7) Fronko, R. M.; Penner-Hahn, J. E.; Bender, C. J. *J. Am. Chem. Soc.* **1988**, *110*, 7554.
(8) Degischer, G.; Nancollas, G. N. *Inorg. Chem.* **1970**, *9*, 1259.
(9) Chaberek, S., Jr.; Martell, A. E. *J. Am. Chem. Soc.* **1952**, *74*, 6228–6231.
(10) Rush, J. D.; Bielski, B. H. J. *J. Phys. Chem.* **1985**, *89*, 5062.
(11) Schwarz, H. A. *J. Chem. Educ.* **1981**, *58*, 101.
(12) Buxton, C. V. *Radiation Chemistry, Principles and Applications*; Farhataziz, Rogers, M. A. J., Eds.; VCH: New York, 1987; pp 321–349.
(13) Irvine, M. J.; Wilson, I. R. *Aust. J. Chem.* **1979**, *32*, 2283.
(14) Cooper, S. R.; Klein, M. *J. Am. Chem. Soc.* **1977**, *99*, 6624.
(15) Bielski, B. H. J.; Allen, A. O. *J. Phys. Chem.* **1967**, *71*, 4544.
(16) Bielski, B. H. J.; Cabelli, D. E.; Arudi, R.; Ross, A. B. *J. Phys. Chem. Ref. Data* **1985**, *14*, 1041–1100.

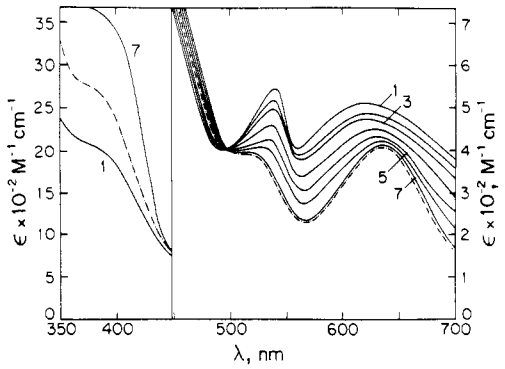

Figure 1. UV-visible absorption spectrum of the $Mn^{III,IV}$edda dimer (curve 1) and the pH dependence of solution spectra between pH 4.2 and 6.5. The spectra of pH <6 correspond to the sum of Mn^{III}edda and Mn^{IV}edda absorbances at pH (curve 1) 6.45, (curve 3) 5.93, (curve 5) 5.45, (curve 7) 4.9. The dotted and dashed curve is the spectrum at pH 4.2.

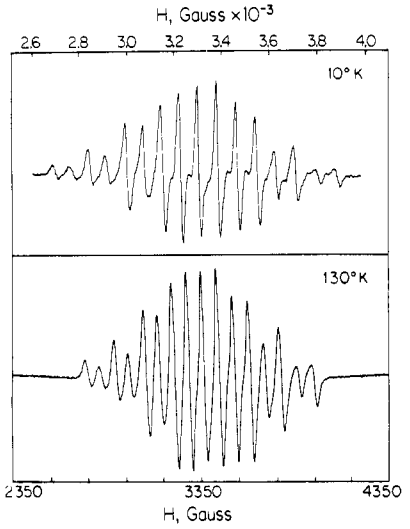

Figure 2. ESR spectra of $Mn^{III,IV}$edda in frozen water at pH 6.5 at 10 K (upper) and at 130 K (lower). The 10 K spectrum was obtained at 9.26 GHz (note different scale) and the 130 K spectrum at 9.45 GHz with 2 mW microwave power. Both spectra are centered at $g = 2.0$. Spectral widths are 1280 G and hyperfine coupling constants are $A_1 \cong 160$ G and $A_2 \cong 80$ G.

bipyridine complex. The signal shown in Figure 2 is representative of Mn(III,IV) dinuclear systems.[3] The hyperfine coupling constants for two nuclei of spin $I_s = {}^5/_2$ are, by inspection, $A_1 \cong 160$ G and $A_2 \cong 80$ G within a range typical of the μ-oxo-bridged systems with amine/carboxylate ligands. At 10 K, the spectral line widths narrow and features due to a small g-anisotropy can be distinguished (Figure 2). The spectrum is not detected above 190 K.

The pH dependence of the ESR signal intensity is shown in Figure 3, coplotted with the absorption measured at 380 nm. The speciation calculated from the absorption data is slightly different from the ESR signal strength, which exhibits a limiting second-order dependence on $[H^+]$ and is analogous to that observed in the dissociation of the bis(μ-oxo)-bridged $Mn^{III,IV}$bpy complex.[14] Accordingly, we propose an analogous structure for the edda complex in reaction 1. The discrepancy between ESR and absorption data probably reflect further protonations of the mononuclear species. From the former, $K_1 = 10^{-10.2}$ M^{-1}. The charges on the species in eq 1 are speculative. No ESR signal for the mononuclear Mn(IV) complex was detected in the $g = 2$ region, but this may be overlaid (or identical with) a signal from manganous ions.

$$[(\text{edda})Mn^{III}(\mu\text{-O})_2Mn^{IV}(\text{edda})]^- + 2H_3O^+ \underset{}{\overset{K_1}{\rightleftharpoons}} Mn^{III}\text{edda}(H_2O)_2^+ + Mn^{IV}\text{edda}(OH)_2 \quad (1/-1)$$

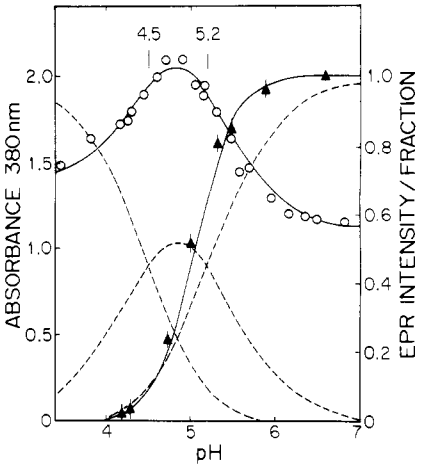

Figure 3. Speciation of Mn^{III}/Mn^{IV}edda as shown by optical density changes at 380 nm (○) and by ESR relative intensity (▲). The optical data are consistent with pK_a's (4.5 and 5.2), giving rise to three hydrolytic forms with the speciation indicated by the dashed lines. The ESR data is fitted to eq 1 in the text, consistent with simple dissociation of the mixed-valence complex.

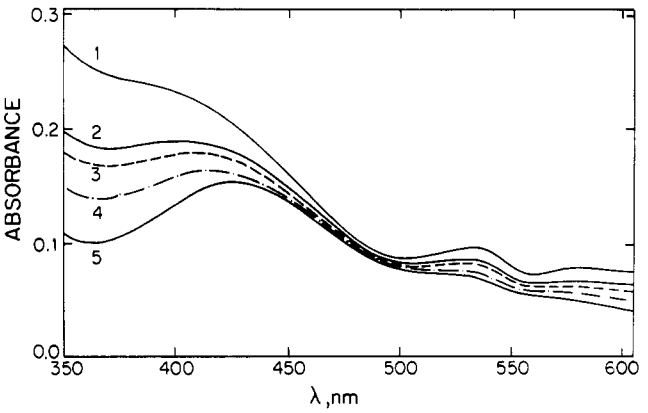

Figure 4. Absorption spectra of solutions containing 6.2 (±0.2) × 10^{-4} M total manganic ($[Mn(III)]_T$) and Mn^{II}edda concentrations (curves 1–5): 2 × 10^{-4}, 9 × 10^{-4}, 1.8 × 10^{-3}, 3.6 × 10^{-3}, 0.018 M. Solutions were buffered with 0.02 M edda at pH 6. The calculated ratios of $[Mn^{III,IV}\text{edda}]/[Mn^{III}\text{edda}]^2$ are given in Table 2B.

Table I. Dependence on $[H^+]$ of the Rates of Dissociation of $Mn^{III,IV}$edda in 0.1 M $NaOAc/HClO_4$

pH	k_{obs}, s^{-1}	pH	k_{obs}, s^{-1}
3.65	1.75	4.3	0.6
3.8	1.3	4.6	0.25
4.0	1.0	5.2	0.1

The rate at which the complex dissociates was measured over the pH range 3.6–5.2 and is first order in $[Mn^{III,IV}\text{edda}]$ and in $[H^+]$. Some observed rate values are listed in Table I, from which the overall forward rate of reaction 1, $k_1/[H^+] = 1$ (±0.2) × 10^4 M^{-1} s^{-1} at 0.1 M ionic strength was obtained. The rather slow dissociation kinetics of the oxo bridges support the proposed structure since substitution of bipyridine by edda on $Mn^{III,IV}$bpy is very fast at pH 6.

The $Mn^{III,IV}$edda complex is a weaker oxidant than Mn^{III}edta.[17] It oxidizes iodide very slowly and Mn^{II}edta completely only when the latter is present in excess. Cyclic voltammetry gave irreversible behavior with a reduction wave at 250 mV and oxidation wave at 450 mV vs Ag/AgCl. A lower limit on the one-electron-reduction potential of ~0.4 V vs NHE is suggested by its fast ($k(Mn^{III,IV}\text{edda} + Fe(CN)_6^{4-}) = 3.2 \times 10^4$ M^{-1} s^{-1}) and irreversible oxidation of ferrocyanide at 0.1 M ionic strength. The

(17) (a) Hamm, R. E.; Suwynn, H. A. *Inorg. Chem.* **1967**, *6*, 139. (b) Yoshino, Y.; Ouichi, A.; Tsunoda, Y.; Kujina, M. *Can. J. Chem.* **1962**, 90, 175.

Table II. Equilibrium of $Mn^{III,IV}$edda and Mn^{III}edda

(A) Values of K_D ($[Mn(III,IV)]/[Mn(III)]^2$) at $[Mn^{II}edda] = 0.01$ M, pH 6.05, and $[Mn(III)]_T = 3[Mn(III,IV)] + [Mn(III)]$

$10^4[Mn(III)]_T$,[a] M	$10^4[Mn(III)]_T$,[b] M	$10^{-3}K_D$,[b] M^{-1}
4.0	4.2	0.63
7.6	5.4	1.7
11.0	9.8	0.94
24.8	24.5	1.2
30.4	30.8	1.95

mean stoichiometry, $([H_2O_2]/[Mn(III)]_T) = 0.45$
mean $K_D = 1.1(\pm 0.4) \times 10^3$ M^{-1}

(B) Dependence of K_D on [Mn(II)], pH 6.05, $[Mn(III)]_T = 6.2(+0.2) \times 10^{-1}$ M

10^3[Mn(II)], M	$10^{-4}K_D$,[b] M^{-1}	$10^4[Mn(III)]_T$, M	K_D[Mn(II)]
0.2	10.0	6.4	20.0
0.9	2.1	5.8	18.9
1.8	0.31	6.3	5.5
3.6	0.15	6.6	5.4
10.0	0.11	6.0	11
18.0	0.045	5.6	8.0

[a] $2[H_2O_2]$. [b] Calculated.

formal three-electron-reduction potential at pH 6.7 was found to be $E°'(Mn^{III,IV}edda/3Mn^{II}edda) = 0.3$ (±0.03) V vs Ag/AgCl. Dissociation of the complex, however, greatly increases the oxidizing strength of solutions.

In neutral solutions, the complex is unstable unless some Mn^{II}edda is present. Increasing the concentration of Mn^{II}edda causes the spectral changes shown in Figure 4. The final spectrum is that of Mn^{III}edda (probably $Mn^{III}edda(OH)_2^-$ at these pH's) as determined by pulse radiolysis (vide infra). The relevant redox and association reactions appear to be eq 2–4. Only reaction 4

$$2Mn^{III}L \rightleftharpoons Mn^{II}L + Mn^{IV}L \quad (2)$$

$$Mn^{IV}L + Mn^{III}L \rightarrow Mn^{III}Mn^{IV}L_2 \quad (3)$$

$$Mn^{II}L + Mn^{III}Mn^{IV}L_2 \xrightarrow{k_4} 3Mn^{III}L \quad (4)$$

can be measured directly. However, the equilibrium amounts of the absorbing species Mn^{III}edda and $Mn^{III,IV}$edda can be measured by analysis of the solution spectra at pH >6. At a given concentration of Mn(II), the ratio $[Mn(III,IV)]/[Mn(III)]^2$ ($=K_D$) is found to be essentially independent of the total concentration of higher valent manganese. However, K_D itself depends inversely on [Mn(II)] and from the approximate relation $K_D = 11$ (±3)/[Mn^{II}edda] the equilibrium concentrations of Mn^{III}edda and $Mn^{III,IV}$edda are calculable. These observations are roughly consistent with eqs 2–4 and are summarized in Table II where values of K_D are listed for solutions containing constant [Mn^{II}edda] and variable total manganic concentration (Table IIA and constant total manganic concentration with variable [Mn^{II}edda] (Table IIB).

The Oxidation of Mn^{II}edda by Hydrogen Peroxide. Kinetics. The oxidation of Mn^{II}edda to $Mn^{III,IV}$edda is the reaction that is primarily responsible for catalase activity. The reaction is autocatalytic and follows the rate law

$$\frac{d[Mn^{III,IV}edda]}{dt} = k_5[Mn^{III,IV}edda][Mn^{II}edda] \quad (5)$$

As indicated by eq 5, the rate is independent of peroxide concentration. If manganic ions are not initially present, an induction period precedes the formation of the mixed-valence complex. The rate constant $k_5 = 50$ (±5) M^{-1} s^{-1} was evaluated over a 10-fold range (0.5–5 mM) of Mn^{II}edda concentrations by simulation of spectrophotometer traces similar to those shown in Figure 5. Two distinct processes occur when Mn^{II}edda is the excess reagent. The formation of $Mn^{III,IV}$edda is followed by reaction 4 (decreasing absorbance) to an equilibrium with mononuclear Mn^{III}edda. The second phase of the reaction is made more apparent by the use of 0.025 M cacodylate buffer (pH 6.3). The cacodylate ion stabilizes mononuclear manganese(III) but does not affect the

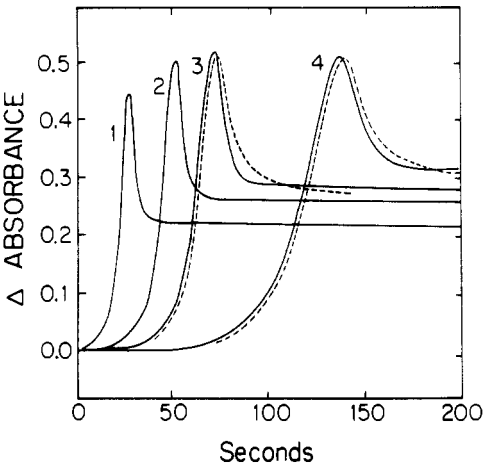

Figure 5. Spectrophotometer traces at 380 nm of the oxidation of Mn^{II}edda by hydrogen peroxide (0.5 mM) in 0.025 M sodium cacodylate (pH 6.3) buffer. The initial concentrations of manganese(II) are as follows: for trace 1, 10 mM; for trace 2, 6 mM; for trace 3, 4 mM; for trace 4, 2 mM. The initial rise and then decrease of absorbance represents the formation of $Mn^{III,IV}$edda followed by equilibration with the mononuclear Mn^{III}edda(cacodylate) complex. Dashed curves are computer simulations of two traces as described in the text.

Table III. Observed Rate Constants for the Reaction[a]

$$Mn^{III,IV}edda + Mn^{II}edda \xrightarrow{\text{cacodylate}} 3Mn^{III}edda(cac)$$

$10^3[Mn^{II}edda]$, M	k_{obs}, s^{-1}	$10^3[Mn^{II}edda]$, M	k_{obs}, s^{-1}
2.0	0.17	6.0	0.43
4.0	0.30	8.0	0.52
5.0	0.35	15.0	0.87

[a] In 0.025 M sodium cacodylate buffer, pH 6.3. $[Mn(III,IV)edda]_0$ was 5×10^{-4} M.

reaction rates at low concentrations. When hydrogen peroxide is in slight stoichiometric excess, formation of $Mn^{III,IV}$edda is nearly quantitative and the kinetic traces are of a typical autocatalytic shape. In Figure 5, the symmetry at the peaks of the absorbance vs time traces suggests that reaction 4 and the rate-determining step in the autocatalytic formation of $Mn^{III,IV}$edda (rate law (5)) occur at the same rate.

Reaction between $Mn^{III,IV}$edda and Mn^{II}edda was measured in the stopped-flow instrument. A cacodylate buffer was used to favor the equilibrium concentration of mononuclear manganese(III) by inhibiting reactions 2 and 3. Observed rate constants, from which $k_4 = 52$ M^{-1} s^{-1} was calculated, are listed in Table III. First-order plots gave an intercept of 0.07 s^{-1}, which indicates a slow reaction between cacodylate and the mixed-valence complex.

The interaction of Mn^{II}edda with the mixed-valence complex in the absence of hydrogen peroxide forms only Mn^{III}edda. The similarity in kinetic order of the autocatalytic oxidation as well as the rate constants k_4 and k_5 strongly suggests that there exists an intermediate common to both processes that is very rapidly oxidized by a peroxide. This may involve an adduct (formally $Mn^{III}{}_3L_3$) as postulated in reactions 6–8 (L = edda).

$$Mn^{II}L + Mn^{III}Mn^{IV}L_2 \xrightarrow{k_6} Mn^{III}{}_3L_3 \xrightarrow{k_{6'}} 3Mn^{III}L \quad (6,6')$$

$$Mn^{III}{}_3L_3 + H_2O_2 \xrightarrow{k_7} [Mn^{III}Mn^{IV}\cdot Mn^{IV}]L_3 + H_2O \quad (7)$$

$$[Mn^{III}Mn^{IV}\cdot Mn^{IV}]L_3 \xrightarrow{k_8} Mn^{III}Mn^{IV}L_2 + Mn^{IV}L \quad (8)$$

Under experimental peroxide concentrations (≥0.1 mM), the rate of reaction 7 exceeds that of reaction 6′ accounting for the biphasic kinetic behavior. The system of eqs 4–8 was used to simulate the traces shown in Figure 5, assuming $k_7[H_2O_2] \gg k_{6'}$. All reactions subsequent to formation of $Mn^{III}{}_3L_3$ are fast, and it is possible that the product of reaction 7 reacts directly with Mn^{II}edda rather than dissociating to free Mn(IV). There were

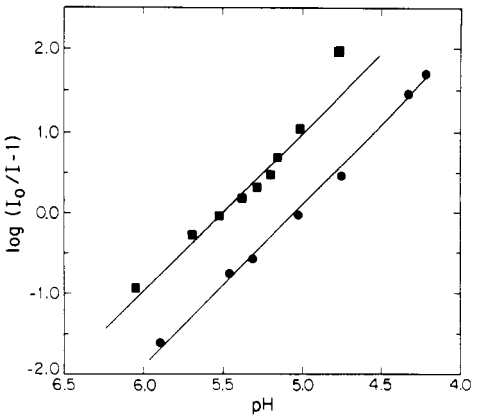

Figure 6. pH dependence of the rate of $Mn^{III,IV}$edda formation (■) and ESR signal intensity (●). $I = d[Mn(III,IV)]/dt$ measured at the asymptote of autocatalytic traces or the signal intensity and I_0 are these values at $6.5 < pH < 7$ in which range they are constant. The abscissa function vs pH is derived for an equilibrium, $I = I_0(1 + K[H^+]^n)^{-1}$ where only the deprotonated forms contribute to rate/signal intensity.

no spectral indications of binding between H_2O_2 and $Mn^{III,IV}$edda.

The possible role of peroxide binding was investigated by substituting the hindered alkyl peroxides *tert*-butyl hydroperoxide and di-*tert*-butyl peroxide for H_2O_2. Mn^{II}edda is oxidized autocatalytically to $Mn^{III,IV}$edda by *tert*-butyl hydroperoxide according to the rate expression $d[Mn(III,IV)]/dt = k[Mn(II)][Mn(III,IV)][(CH_3)_3COOH]$, where $k \cong 110\ M^{-2}\ s^{-1}$. A small amount of added manganic acetate is necessary to initiate the reaction. The dependence on oxidant concentration suggests that, in contrast to H_2O_2, the proposed $Mn^{III}_3L_3$ intermediate dissociates faster than it is oxidized by the alkyl hydroperoxide and this reaction occurs at less than 0.1% the rate of H_2O_2 oxidation in reaction 7. Di-*tert*-butyl peroxide is entirely inert as an oxidant.

Effect of Inhibitors. The effects of hydroxyl radical and superoxide scavengers on the autocatalytic reaction were determined. The former (e.g. salicylate, *tert*-butyl alcohol, and formate) had no effect upon the autocatalytic processes but tended to prolong the induction period. In deaerated 0.1 M formate solutions, a condition under which hydroxyl radicals produce the reducing radical CO_2^-, no reaction occurred for 30 min after mixing or until a small amount of $Mn^{III,IV}$edda was added after which the reaction proceeded without inhibition. Oxygen also had no effect upon the rates or overall stoichiometry. This suggests that small manganic concentrations accumulate by a slow one-electron reduction of peroxide during the induction period until sufficient to initiate autocatalysts.

Tetranitromethane (TNM), an efficient scavenger of O_2^- radicals, slowed the reaction and reduced the amount of $Mn^{III,IV}$edda formed autocatalytically by about 50% when peroxide was the limiting reagent. This seems attributable to the scavenging of superoxide radicals or superoxide complexes[18] produced by a reaction between H_2O_2 and manganese(IV). In the absence of TNM, these radicals are probably reduced by Mn^{II}edda as in eqs 9 and 10. Under most conditions, these may be considered as

$$Mn^{IV}L + H_2O_2 \rightarrow [Mn^{III}L(O_2^-)] \rightleftharpoons Mn^{III}L + O_2^- + 2H^+ \quad (9)$$

$$O_2^- + Mn^{II}L + 2H^+ \rightarrow Mn^{III}L + H_2O_2 \quad (10)$$

side reactions since no net change in the oxidation state of manganese results. The details of these processes were investigated by pulse radiolysis (vide infra).

pH Dependence of the Autocatalytic Reaction. The rate of the autocatalytic oxidation of Mn^{II}edda to $Mn^{III,IV}$edda is closely related to the equilibrium of eq 1. At pH <6, both the rate (measured as the maximal rate of absorbance increase at 380 nm) and the final concentration of Mn(IV)-containing complexes decreased. The edda ligand (0.01 M) was used to buffer the reaction and keep Mn^{2+} fully complexed. In Figure 6, the rate of the autocatalytic reaction (relative to its maximal rate) is shown coplotted with the same function of ESR relative signal intensity (I/I_0). The slope of the function log $[(I_0/I) - 1]$ vs pH in both cases is 2, the order of the proton dependence, and the intercept at $[H^+] = 0$ corresponds to K_1 for the ESR data but is slightly smaller ($10^{-11}\ M^{-1}$) for the rate data. This result verifies that only the dinuclear complex can act as a catalyst for peroxide reduction. The shift in K_1 calculated from the rate data seems to be due to the instability of mononuclear Mn(IV) at lower pH's.

Table IV. Rate Data for Reactions of Superoxide with Mn^{II}edda and Mn^{III}edda

(a) Reaction 11: $Mn^{II}edda + O_2^- \rightarrow Mn^{III}(O_2^{2-})edda$, pH 7.1, $\mu = 0.1$ M

$10^4[Mn^{II}edda]$, M	$10^{-4}k_{obs}$, s^{-1}	$10^4[Mn^{II}edda]$, M	$10^{-4}k_{obs}$, s^{-1}
2.0	3.4	0.1	0.15
1.0	1.7		

(b) Reaction 12: $Mn^{III}(O_2^{2-})edda \rightarrow Mn^{III}edda + H_2O_2$ pH 6.3, $k_{12} = 220\ (\pm 20)\ s^{-1}$; pH = 7.1, $k_{12} = 50\ (\pm 5)\ s^{-1}$

(c) Reaction 13: $Mn^{III}edda + O_2^- \rightarrow Mn^{II}edda + O_2$, pH 7.1, $\mu = 0.1$ M (formate)

$10^5[Mn^{III}edda]$, M	k_{obs},[a] s^{-1}	$10^5[Mn^{III}edda]$, M	k_{obs},[a] s^{-1}
0.5	14	4.0	52
1.0	25	6.0	50
2.0	40	8.0	55
3.0	48		

[a] Observed rates were measured at doses of 2–10 μM O_2^- and extrapolated to $[O_2^-]_0 \rightarrow 0$ to account for the spontaneous rate of O_2^- dismutation.

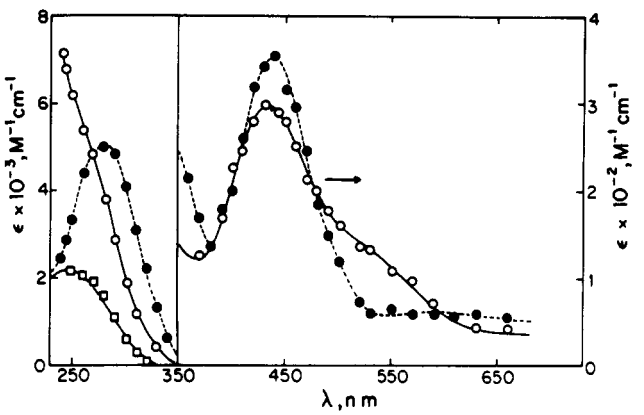

Figure 7. Absorption spectra of transients formed in the oxidation of Mn^{II}edda by superoxide anion at pH 6–7, in oxygen-saturated 0.01 M sodium formate solution. Shown, in sequence of their formation after the pulse, are the spectra of (□) superoxide, (●) $Mn^{III}(O_2^{2-})$edda, and (○) mononuclear Mn^{III}edda.

Reaction of Superoxide Radicals with Mononuclear Mn^{II}edda and Mn^{III}edda Complexes. The effect of TNM upon the autocatalytic reaction caused us to investigate the possible involvement of superoxide radicals or their metal complexes. It was also necessary to confirm the spectral characteristics of mononuclear Mn^{III}edda. Superoxide radicals were generated as described in the Experimental Section in the presence of Mn^{II}edda. These radicals oxidize Mn(II) to Mn(III) via a transient superoxo–Mn(II) or peroxo–Mn(III) transient such as have been observed in other systems.[19] Rate data for reactions 11 and 12 are

$$Mn^{II}edda(H_2O)_2 + O_2^- \xrightarrow{k_{11}} [Mn^{III}edda(O_2^{2-})]^- \quad (11)$$

$$[Mn^{III}edda(O_2^{2-})]^- + 2H_2O \xrightarrow{k_{12}} [Mn^{III}edda(OH)_2]^- + H_2O_2 \quad (12)$$

(18) (a) Rush, J. D.; Bielski, B. H. J. *J. Phys. Chem.* **1985**, *89*, 1524. (b) Ryvkina, L. S.; Berdnikov, V. M. *React. Kinet. Catal. Lett.* **1982**, *21*, 409.

presented in Table IV, and the electronic spectra of the transient complex and mononuclear Mn^{III}edda are shown in Figure 7. At pH 7.1, $k_{11} = 3 \times 10^7\ M^{-1}\ s^{-1}$ and $k_{12} = 50\ s^{-1}$. The similar visible absorptions of the products of both species indicate that the transient is correctly formulated as a manganese(III) peroxo complex. A shoulder at ~530 nm in the final product is absent in the peroxo complex. This feature is very prominent in the mixed-valence complex and appeared in other Mn^{III}edda derivatives. It may be associated with oxide or hydroxide ligands that are substituted by a side-on bound peroxide ligand in Mn^{III}edda$(O_2^{2-})^-$. The conformation of edda on Mn(III) is uncertain (three isomers are possible), but studies of trivalent cobalt complexes indicate that trans glycinate rings above and below the diammine bridge are the preferred orientation.[20] This tendency should be enhanced in hydrolyzed forms of Mn^{III}edda where stronger field amine and hydroxide ligands are expected to occupy equatorial sites in a Jahn–Teller distorted system.

The rate of dissociation of the peroxide complex is unaffected by excesses of Mn^{II}edda up to 0.01 M. We could ascertain no evidence of further reactivity for this species as it might apply to the autocatalytic reaction.

Superoxide radicals bind with and are oxidized by Mn^{III}edda$(OH)_2^-$. To measure this process, Mn^{II}edda was completely oxidized by large pulses of O_2^- radicals followed quickly by a smaller pulse in which the decay kinetics of O_2^- were measured. These first-order decay rates are listed in Table IV and show saturating behavior at $[Mn^{III}edda] > 3 \times 10^{-5}$ M. Reactions 13 and 14, $K_{13} = 3 \times 10^4\ M^{-1}$ and $k_{14} = 55\ (\pm 5)\ s^{-1}$, are consistent

$$Mn^{III}edda(OH)_2^- + O_2^- \overset{K_{13}}{\rightleftharpoons} [Mn^{III}edda(OH)_2O_2^-]^{2-} \quad (13)$$

$$[Mn^{III}edda(OH)_2(O_2^-)] + 2H^+ \xrightarrow{k_{14}} Mn^{II}edda(H_2O)_2 + O_2 \quad (14)$$

with these observations. The spectral properties of the intermediate were difficult to determine owing to the high background absorption on Mn^{III}edda but resemble a superposition of the superoxide and Mn^{III}edda spectra shown in Figure 7. The characteristic bands above 500 nm of Mn^{IV}edda were not observed. The high binding constant of reaction 13 was unexpected, but taken together reactions 11–14 are consistent with the earlier reported superoxide dismutase activity of Mn^{II}edda solutions.[21]

Reactions of Dinuclear $Mn^{III,III}$edda. Spectral measurements (Figure 4) indicated that dinuclear $Mn^{III,IV}$edda and mononuclear Mn^{III}edda are the major equilibrium solution species. However, Mn^{III}edda is expected to form dimers prior to disproportionation, and in order to determine the spectral properties and kinetic stability of dinuclear $Mn^{III,III}$edda, $Mn^{III,IV}$edda was reduced by formate (CO_2^-) radicals and the aquated electron. Reaction 15

$$[LMn^{III}O_2Mn^{IV}L]^- \xrightarrow{CO_2^-/e_{aq}^-} [LMn^{III}O_2Mn^{III}L]^{2-} \quad (15)$$

$$[LMn^{III}O_2Mn^{III}L]^{2-} \xrightarrow{k_{16}} Mn^{II}L + Mn^{IV}L \quad (16)$$

was complete within about 100 μs of the pulse. The negative change in absorbance was subtracted from the spectrum of $Mn^{III,IV}$edda to obtain the spectrum of the corresponding (III,III) system shown in Figure 8. This spectrum is similar to those of some cationic μ-oxo- and μ-acetato-bridged Mn(III) dimers with amine ligands.[3a,c] The manganic dimer undergoes a slow first-order reaction ($k_{16} \cong 0.3\ s^{-1}$) to yield manganese(IV), which is detected by a partial restoration of the initial absorbance near 600 nm.

Dinuclear $Mn^{III,III}$edda is evidently not a significant solution species because of reaction 16, but its kinetic stability is such that a multinuclear Mn(III) species is a plausible intermediate in the autocatalytic mechanism.

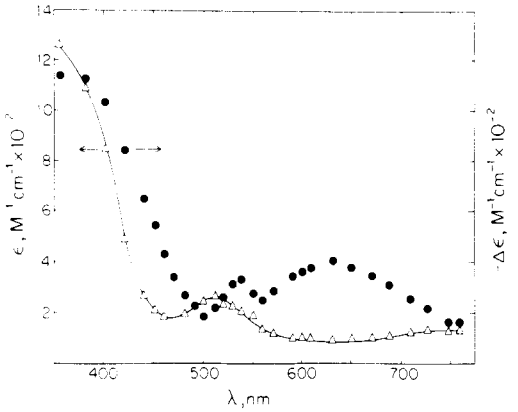

Figure 8. Spectrum of dinuclear $Mn^{III,III}$edda formed by reduction of $Mn^{III,IV}$edda (~1 mM) with CO_2^-/e_{aq}^- in argon-saturated, 0.01 M formate solution at pH 6.1. The calculated points (Δ) are obtained by subtraction from the spectrum in Figure 1 of the observed change in extinction after the pulse (●) assuming $G(Mn^{III,IV}edda) = 6$.

Table V. Dependences of Rates of Hydrogen Peroxide Decomposition on Concentrations of $Mn^{II,III}$edda and H_2O_2 and pH

(a) $[Mn^{II}edda] = 4 \times 10^{-4}$ M, pH 7

$[H_2O_2]$, M	$10^{-4}(d[H_2O_2]/dt)_0$, M s^{-1}	$[H_2O_2]$, M	$10^{-4}(d[H_2O_2]/dt)_0$, M s^{-1}
0.035	0.79	0.20	5.1
0.05	1.2	0.50	12.3
0.10	2.6		

(b) $[H_2O_2] = 0.1$ M, pH 7

$10^4[Mn^{II}edda]_0$, M	$(d[H_2O_2]/dt)_0$, M s^{-1}	$10^4[Mn^{II}edda]_0$, M	$(d[H_2O_2]/dt)_0$, M s^{-1}
2	0.92	8	4.0
4	2.2	16	8.7

(c) pH Dependence of k_{17}

pH	k_{17}, $M^{-1}\ s^{-1}$	pH	k_{17}, $M^{-1}\ s^{-1}$
7.1	5.4	5.4	2.15
6.5	4.2	5.15	0.0
5.75	3.0	4.8	0.0

The dimerization of Mn^{III}edda was not measurable directly though the formation of the mixed-valence complex from manganic acetate, as well as the induction period prior to autocatalysis, suggests that it occurs. The Fe^{III}edda complex dimerizes, and from spectrophotometric measurements $K(2Fe^{III}L \rightleftharpoons Fe_2^{III}L_2) = 7.5\ (\pm 1.5) \times 10^2\ M^{-1}$ in 0.02 M edda buffers at pH 6–6.5. A similar value for Mn^{III}edda would be compatible with the above observations.

Catalase Activity of Mn(edda) Complexes. A small amount of solid Mn^{II}edda dissolved in 1 M H_2O_2 causes the vigorous evolution of dioxygen, during and after which no trace of manganic hydroxide precipitates are observed. At somewhat lower peroxide (or higher Mn(II)) concentrations the green color of the $Mn^{III,IV}$edda complex is visible during peroxide disproportionation. Its steady-state concentration is oscillatory in unbuffered solutions as described below. The rate of the catalytic disproportionation of H_2O_2 to oxygen and water is first-order in both peroxide and manganese edda concentrations (rate law (17)). The initial rates

$$-\frac{d[H_2O_2]}{dt} = k_{17}[Mn^{II}edda]_0[H_2O_2] \quad (17)$$

of peroxide disappearance as a function of $[Mn^{II}edda]$ and $[H_2O_2]$ are listed in Table V. At pH 7, $k_{17} = 5.4\ M^{-1}\ s^{-1}$. Also from Table V, k_{17} is a weak function of pH in the range pH 5.4–7.1 but goes essentially to zero below pH 5.2. The rate law for peroxide decomposition when $[H_2O_2] \gg [Mn^{II}edda]_0$ (eq 17) compared to that when $[Mn^{II}edda]_0 > [H_2O_2]$, essentially eq 5, suggests that hydrogen peroxide reduces a transient or product of reactions 6–8 to establish a steady-state ratio of Mn^{II}edda/$Mn^{III,IV}$edda during catalase activity.

(19) (a) Cabelli, D.; Bielski, B. H. J. *J. Phys. Chem.* **1984**, *88*, 3111, 6291–6294. (b) Lati, J.; Meyerstein, D. *J. Chem. Soc., Dalton Trans.* **1978**, 1105.
(20) Coleman, P. F.; Legg, J. I.; Steele, J. *Inorg. Chem.* **1970**, *9*, 937.
(21) Koppenol, W. H.; Levine, F.; Hatmaker, T. L.; Epp, J.; Rush, J. D. *Arch. Biochem. Biophys.* **1986**, *251*, 594–599.

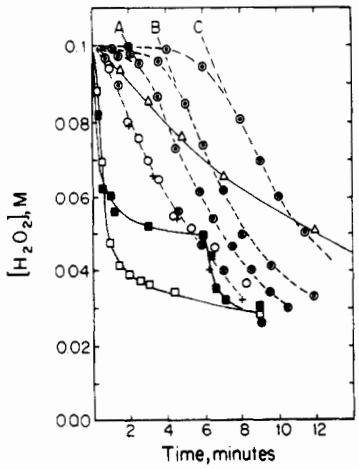

Figure 9. Time dependence of H_2O_2 decomposition catalyzed by 0.4 mM Mn^{II}edda in the presence of (○) 0.2 M *tert*-butyl alcohol, (+) 0.2 M $LiClO_4$, (⊙) [TNM] = (A) 0.4, (B) 0.8, or (C) 1.2 mM, (△) 0.1 M phosphate, or (□) 0.5 M sodium azide. All solutions were maintained at pH 7 and with $[edda]_0$ = 0.01 M. In one run (■) containing azide, the total amount of 0.01 M edda was reached by 5 mM increments of edda, added initially, and then added after catalase activity had terminated.

Ligand Oxidation. During catalase activity, edda is consumed, and reaction ceases after it is entirely oxidized. The efficiency of the reaction, as moles of H_2O_2 decomposed per mole of edda rendered inactive, is directly proportional to the initial $[H_2O_2]$. When $[H_2O_2]_0$ was varied over the range from 0.05 to 0.5 M at fixed concentrations of edda (2.5×10^{-3} M) and Mn(II) (4×10^{-4} M), the turnover efficiency increased from 10 (0.05 M) to 100 (0.5 M), indicating that the oxidizing species is competitively reduced by H_2O_2 and by the edda ligand. In effect, regardless of $[H_2O_2]_0$, the same fraction of H_2O_2 is decomposed before ligand decomposition terminates the reaction. Catalase activity is immediately resumed after addition of fresh ligand. Isolation of the oxidized ligand from concentrated solutions gave a tarlike product. In the presence of ferric ions this material developed a violet hue, suggesting that hydroxamates are among the oxidation products.

Effects of Inhibitors and Accelerators. The rate law of eq 17, with direct dependences on [Mn(edda)] and $[H_2O_2]$, reflects the respective phases of catalase activity in which hydrogen peroxide is reduced to water and oxidized to dioxygen. The pH dependence described above largely reflects the pH sensitivity of the reductive phase, which is the autocatalytic reaction. Similarly, additives that affect reactions 6–8 generally affect catalase activity. Catalase activity is inhibited by TNM, but not by *tert*-butyl alcohol or other hydroxyl radical scavengers. Activity is independent of ionic strength. Phosphate ion (0.1 M) reduces the rate of peroxide decomposition by a factor of 2 analogous to its effect upon the autocatalytic reaction. These experimental results are summarized in Figure 9.

The oxidative phase cannot be studied independently of catalase action. The competition between ligand and peroxide oxidation indicates that the primary oxidant is not $Mn^{III,IV}$edda, which is stable and degraded very slowly by excess H_2O_2. Also, peroxide is oxidized directly to dioxygen, especially in more concentrated peroxide solutions. Nitro-blue tetrazolium (NBT), a superoxide scavenger that produces intensely purple formazan upon reduction by O_2^-, had no reaction during the vigorous decomposition of 1 M hydrogen peroxide by Mn^{II}edda. NBT is a more selective scavenger than TNM, and concentrations of 3–5 mM were used to make its potential reaction with O_2^- competitive with reaction 11 of Mn^{II}edda at a concentration of 0.2 mM. Fe^{III}edda, an O_2^- generator via Fenton-related reactions, having much weaker catalase activity than Mn^{II}edda, immediately gave precipitates of formazan under the same conditions, as did suspensions of manganese dioxide.

An additional probe of the peroxide-oxidizing transient is the effect of azide ion. The original identification of non-heme catalases in bacteria arose from their insensitivity to azide ions that completely inhibit heme catalases.[22] Azide binds weakly (K_{assn} = 11 (± 2) M^{-1}) with $Mn^{III,IV}$edda to give an orange complex. The 16-line ESR signal is unaffected but the adduct is less stable to reduction than the uncoordinated species. High concentrations of azide accelerate the rate of peroxide decomposition and of ligand degradation. As shown in Figure 9, in the presence of 0.5 M N_3^- the rate of increase of peroxide is about 5 times as rapid as in solutions containing no azide, but the efficiency with respect to ligand oxidation is lower. Measurements with an oxygen electrode showed that N_3^- acts as a sacrificial reductant. Over the approximate binding range of $[N_3^-]$, 0.01–0.5 M, oxygen evolution is increasingly replaced by nitrogen evolution. At $[N_3^-]$ = 0.5 M and $[H_2O_2]_0$ = 0.01 M, virtually all peroxide is decomposed reductively. Azide radicals are not formed since, in solutions saturated with acrylonitrile, polymerization was not initiated.

The most competent oxidant of N_3^- or H_2O_2 is not $Mn^{III,IV}$edda but one of the higher valent products of reaction 7 or 8. For the trinuclear intermediate, $Mn^{III,IV,IV}$edda, reactions 18–20 are

$$Mn^{III}Mn^{IV}{}_2L_3 + N_3^- \rightleftharpoons Mn^{III}Mn^{IV}{}_2L_3(N_3^-) \quad (18)$$

$$Mn^{III}Mn^{IV}{}_2L_3(N_3^-) + N_3^- \rightarrow Mn^{III}{}_2Mn^{IV}L_2 + Mn^{II}L + 3N_2 \quad (19)$$

$$Mn^{III}Mn^{IV}{}_2L_3 + H_2O_2 \rightarrow Mn^{III}{}_2Mn^{IV}L_2 + Mn^{II}L + O_2 \quad (20)$$

compatible with our observations. The oxidation of two azides to nitrogen by prior formation of an azido complex has been described in the reaction of Ag(III) with N_3^-.[23]

Oscillations[24] in the Steady-State Concentration of $Mn^{III,IV}$edda. In solutions unbuffered with excess ligand, the natural pH of the Mn^{II}edda complex is about 6.1. The addition of an excess of hydrogen peroxide causes an initial increase in concentration of $Mn^{III,IV}$edda with a corresponding decrease in pH. The dinuclear complex is then partially reduced with a reversal in the direction of pH change. Following a period during which pH remains fairly constant, and peroxide is decomposed, the concentration of $Mn^{III,IV}$edda again increases and then falls. Concurrent plots of absorbance, pH, and $[H_2O_2]$ for this cycle are shown in Figure 10. The oscillations were confirmed by measurements of current generated over a range of constant applied potentials. The magnitude of the cathodic current at a potential of 0.31 V vs Ag/AgCl is also plotted in Figure 10.

The oscillations are qualitatively explicable on the basis of reactions described above. The protons generated by the autocatalytic formation of $Mn^{III,IV}$edda cause the reaction to "overshoot" into the region near pH 5 where the complex is unstable to dissociation (reaction 1) and autocatalysis is inhibited. The reduction of $Mn^{III,IV}$edda after its initial formation probably reflects its rate of dissociation in reaction 1. The final pulse of $Mn^{III,IV}$edda formation occurs as peroxide is nearly depleted. The turnover of peroxide does not reach a true steady state of reduction and oxidation because the autocatalytic formation of $Mn^{III,IV}$edda is independent of $[H_2O_2]$ whereas the reduction to manganese(II) depends directly upon it. Therefore, the former process predominates at the end. The reason for the final decrease is unclear, though it may relate to ligand oxidation.

Discussion

Scheme I summarizes the reactions that are probably most significant in the catalase action. A trinuclear species, formally $Mn^{III}Mn^{IV}{}_2L_3$, is represented as the principal oxidant of hydrogen peroxide. $Mn^{III,IV}$edda is most likely formed by dissociation of $Mn^{III}Mn^{IV}{}_2L_3$ and subsequent reaction of mononuclear Mn^{IV}edda with Mn^{II}edda under conditions when $[H_2O_2] < [Mn^{II}edda]$. The equilibrium between Mn^{III}edda and the mixed-valence species at the left of Scheme I is arrived at via the first reaction in the cycle (reaction 6) when peroxide is absent. As most of these processes

(22) Johnston, M. A.; Delwiche, E. A. *J. Bacteriol.* **1965**, *90*, 352.
(23) Borish, E. T.; Kirschenbaum, L. J. K. *Inorg. Chem.* **1984**, *23*, 2355.
(24) Degn, H. J. *J. Chem. Educ.* **1972**, *49*, 302.

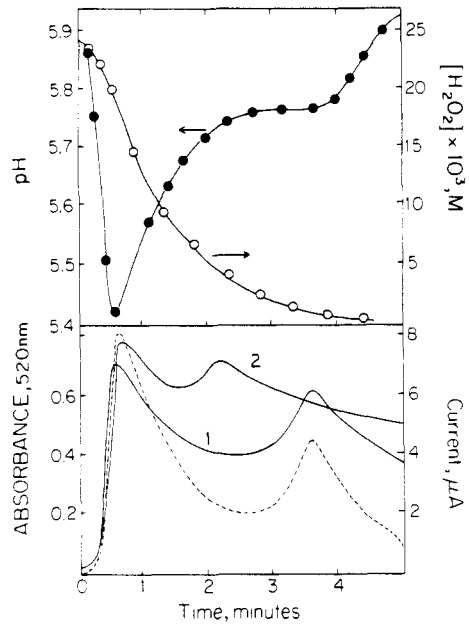

Figure 10. Time dependence of pH and $[H_2O_2]$ (top) and absorbance at 520 nm (bottom, trace 1) during the reaction of 2.5×10^{-2} M H_2O_2 with 6.5×10^{-3} M Mn^{II}edda. Also in the lower figure is the variation in cathodic current (---) during reaction at an applied potential of 0.31 V vs Ag/AgCl. Trace 2 (bottom) shows absorbance changes at a lower $(1.7 \times 10^{-2}$ M) H_2O_2 concentration. As $[H_2O_2]_0$ is decreased to near the stoichiometric level the absorbance "peaks" coalesce.

Scheme I

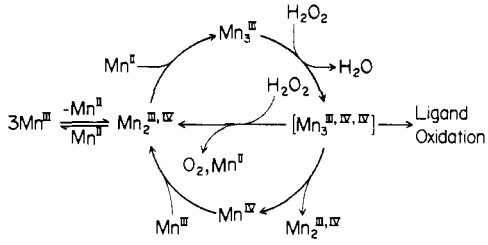

are fast, other kinetically competent mechanisms are possible, but the Scheme I accounts for the essential features. The role of O_2^- remains unclear, though we feel it occurs as a result of side reactions of higher valent manganese with H_2O_2 and is not an essential chain-carrier in the mechanism. Tetranitromethane, which is the only effective inhibitor other than strong reductants such as hydroxylamine, may inhibit by scavenging not only free O_2^- but other transients that support the cycle.

Previous studies of the catalase activity of manganous/histidine solutions[25] proposed a free-radical chain decomposition mechanism. These studies of oxygen evolution were conducted with low Mn(II) concentrations and a large excess of H_2O_2. Histidine lacks a terminal glycinate group, but its donor atoms are similar to edda. In a limited study of this system using higher concentrations of Mn(II) relative to H_2O_2, we observed a similar autocatalytic reaction to form a mixed-valence Mn(III,IV)–histidyl complex. Its optical spectrum resembled that of a more hydrolyzed and unstable form of $Mn^{III,IV}$edda at pH >7.5, but it exhibited the same 16-line ESR spectrum. Therefore, it is likely that in essential respects the catalase mechanisms of these systems are similar.

The two-electron reduction of peroxide is the characteristic reaction of the catalase cycle. Its observable features in the edda system are (1) a rate-determining reaction between Mn^{II}edda and $Mn^{III,IV}$edda that leads to Mn^{III}edda in the absence of peroxide and (2) the necessity that a peroxide have one unhindered –OOH for reaction. In the mechanistic Scheme II, it is proposed that

Scheme II

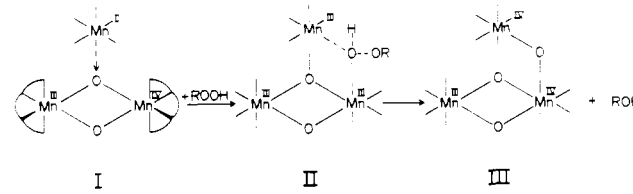

Mn^{II}edda reacts at the oxo bridge of the mixed-valence complex, forming a trinuclear structure that is unstable to dissociation but readily attacked by hydroperoxides (I → II). The peroxide (ROOH; R = H, $(CH_3)_3C$) is cleaved heterolytically, a process in which breaking of the (–O–O–) bond may be facilitated by incorporating one oxygen in a μ-oxo bridge between Mn(IV) atoms in structure III as suggested above. The glycinate bridges are assumed to be substitutable or flexible enough to accommodate expansion of the coordination sphere where necessary.

The associative steps (I and II) would likely involve a large increase in entropy. The ~2-s half-life of dinuclear $Mn^{III,III}$edda in reaction 17 is an upper limit on the life of a trinuclear species. The absence of a hydrogen peroxide dependence in the autocatalytic reaction implies that I → III is a concerted process ($k_7 \geq 10^4$ M^{-1} s^{-1}) provided there is no steric hindrance to peroxide binding with II. The slower reaction and concentration dependence of *tert*-butyl hydroperoxide might be accounted for in this way. It would be unusual for an oxidizing manganese(IV) system to react with peroxides via an oxygen atom transfer rather than a free-radical oxidation to ROO•,[26] and indeed the latter seems to be a competitive reaction. Therefore, the reduction in the oxidation state of the system by addition of Mn(II) is a kinetically and mechanistically plausible precursor to oxidation by ROOH. At present we have no direct evidence for the polynuclear species in Scheme II. For instance, freeze-quenching of reaction mixtures gave only the ESR signal of $Mn^{III,IV}$edda though multinuclear manganic compounds with concatenated oxygen bridges are not uncommon.[27]

An alternate mechanism in which Mn^{II}edda reduces $Mn^{III,IV}$edda to the Mn(III) dimer followed by $LMn^{III}O_2Mn^{III}L + H_2O_2 \rightarrow LMn^{IV}O_2Mn^{IV}L + H_2O$ and other fast reactions could also be constructed. It was pointed out by a reviewer that a binuclear manganese(II) complex catalytically disproportionates hydrogen peroxide by redox cycling through its (II,II) and (III,III) oxidation states.[28] This type of cycle offers clear advantages as a model for an independently functioning active site in a biological catalase. Not enough information on the manganese(III) and manganese(IV) edda dimers could be obtained to fully evaluate the possibility of an analogous (III,III) ⇌ (IV,IV) redox cycle occurring in our system. If active, these species must be present at very low steady-state concentrations during catalase activity. The kinetic data, as well as the visual observation that the mixed-valence complex is the only higher valent manganese present in significant amounts during hydrogen peroxide decomposition, suggest that this species is the catalytic as well as the major equilibrium manganic edda species.

The applicability of Schemes I and II to biological catalases is yet unclear. The edda catalase system is limited by the slow ($k_6 = 52$ M^{-1} s^{-1}) reaction between edda complexes in dilute solution and further by an inefficient reaction between oxidant and H_2O_2. The reason for the latter defect is clarified by the accelerating effect of azide ions. Though azide is not a particularly facile one- or two-electron reductant, its apparent ability to bind directly to $Mn^{III}Mn^{IV}{}_2L_3$ more than compensates for this. Either

(25) (a) Sychev, A. Y.; Isak, V. C. *Russ. J. Phys. Chem. (Engl. Transl.)* **1973**, *47*, 335. (b) Sychev, Y. A.; Isak, V. G. *Russ. J. Phys. Chem. (Engl. Transl.)* **1972**, *46*, 1072.

(26) Challoner, P. A. *Handbook of Coordination Catalysis in Organic Chemistry*; Butterworths: London, 1986; pp 468–473.

(27) (a) Lis, T.; Jezowska-Trzebiatowska, B. *Acta Crystallogr.* **1977**, *B33*, 2112. (b) Baikie, A. R. E.; Hursthouse, M. B.; New, J. B.; Thornton, P. J. *J. Chem. Soc., Chem. Commun.* **1978**, 62. (c) Schake, A. R.; Vincent, J. B.; Li, Q.; Boyd, P. D. W.; Folting, K.; Huffman, J. C.; Hendrickson, D. N.; Christou, G. *Inorg. Chem.* **1989**, *28*, 1915.

(28) Mathur, P.; Crowder, M.; Dismukes, G. C. *J. Am. Chem. Soc.* **1987**, *109*, 5227.

limitation might be removed in a enzymatic catalase using polynuclear active sites or binuclear sites acting cooperatively.

It is relevant to note that catalase activity is partly due to the relatively weak oxidizing properties of $Mn^{III,IV}$edda at pH >6. If H_2O_2 reduced $Mn^{III,IV}$edda easily (as does hydroxylamine), catalase activity would be nil since the trinuclear species derived from the mixed-valence complex via reaction 6 serves as the substrate for peroxide reduction. Other manganic catalases could form the same reactive intermediate(s) by other pathways. A possible test for the occurrence of steps similar to those in Schemes I and II in bacterial catalases would be inhibition or deactivation by reducing agents. Some published experiments on the *Lactobacillus* catalase seem to bear this out[29] though other factors such as loss of manganese might also be involved.

Acknowledgment. This work was supported by a grant from the Council for Tobacco Research Inc., U.S.A. Work done by J.D.R. while at Brookhaven National Laboratory was supported by NIH Grant RO1 GM23656-12. We wish to thank Drs. D. E. Cabelli at BNL for helpful discussions and assistance with pulse-radiolysis experiments and D. F. Church and B. Hales at LSU for assistance with ESR instrumentation.

(29) Kono, Y.; Fridovich, I. *J. Biol. Chem.* **1983**, *258*, 13647.

Contribution from the Department of Applied Chemistry, Faculty of Engineering, Osaka University, Suita, Osaka 565, Japan

Photochemical CO_2 Reduction Catalyzed by $[Ru(bpy)_2(CO)_2]^{2+}$ Using Triethanolamine and 1-Benzyl-1,4-dihydronicotinamide as an Electron Donor

Hitoshi Ishida, Tohru Terada, Koji Tanaka,*,† and Toshio Tanaka

Received July 29, 1988

Irradiation with visible light of a CO_2-saturated triethanolamine (TEOA)/*N*,*N*-dimethylformamide (DMF) solution (1:4 v/v) containing $[Ru(bpy)_3]^{2+}$ and $[Ru(bpy)_2(CO)_2]^{2+}$ (bpy = 2,2'-bipyridine) selectively produced $HCOO^-$ with a maximum quantum yield of 14%. On the other hand, the photochemical CO_2 reduction in CO_2-saturated H_2O/DMF (1:9 v/v) containing $[Ru(bpy)_3]^{2+}$, $[Ru(bpy)_2(CO)_2]^{2+}$, and 1-benzyl-1,4-dihydronicotinamide (BNAH) gave not only CO but also $HCOO^-$ with maximum quantum yields of 14.8 and 2.7%, respectively. In those photochemical CO_2 reductions, the luminescent-state $[Ru(bpy)_3]^{2+*}$ was quenched reductively by TEOA and BNAH, affording $[Ru(bpy)_3]^+$, which functioned as a reductant of $[Ru(bpy)_2(CO)_2]^{2+}$, and the change in the main product from $HCOO^-$ in TEOA/DMF to CO in H_2O/DMF can be explained in terms of the acid-base equilibria among $[Ru(bpy)_2(CO)_2]^{2+}$, $[Ru(bpy)_2(CO)(C(O)OH)]^+$, and $[Ru(bpy)_2(CO)(COO^-)]^+$.

Introduction

Interest in carbon dioxide fixation has increased recently because of its potential use as a C_1 source, the increase of its concentration in air, and efforts to mimic photosynthetic carbon assimilation.[1] Carbon dioxide is reduced at potentials more negative than −2.0 V vs SCE.[2] On the other hand, the reduction of CO_2 occurs at more positive potentials when protons are involved in the reduction. Reductions of CO_2 by means of various electrochemical,[3-14] photoelectrochemical,[15-18] and photochemical[19-28] methods have, therefore, been conducted in the presence of proton donors, where CO_2 is reduced to CO,[3,4,15,22-24,28] HCOOH,[5,6,16,17,19-21,27] HCHO,[18] CH_3OH,[7,11] CH_4,[12,13,25] and other organic compounds.[8,9] Another approach to CO_2 fixation is to activate or reduce organic molecules in order that they will react with CO_2, affording organic acids.[14,26] In such CO_2-fixation reactions, transition-metal catalysts,[3-10,19-25,27,28] semiconductor electrodes,[11,12,15,17,18] or enzymes[16,26] have been used for the activation of either CO_2 or organic molecules.

It is well-known that the reduced form of nicotinamide adenine dinucleotide phosphate (NAD(P)H) plays the role of a reductant in biological CO_2 fixation.[29] In this connection, electron transfer from NAD(P)H model compounds to various substrates has been studied extensively,[30] although no photochemical CO_2 reduction using NAD(P)H model compounds such as 1-benzyl-1,4-dihydronicotinamide (BNAH) has been reported. Among the transition-metal complexes used as catalysts in the photochemical CO_2 reduction,[19-26] $Re(bpy)(CO)_3Cl$ functions not only as a photosensitizer but also as a catalyst in CO_2 reduction.[22] On the other hand, there have been conflicting views with respect to the function of $[Ru(bpy)_3]^{2+}$ in the photochemical CO_2 reduction; an irradiation with light ($\lambda > 320$ nm) of a CO_2-saturated triethanolamine (TEOA)/DMF solution containing $[Ru(bpy)_3]^{2+}$ (0.06 mmol dm^{-3}) and methylviologen has been shown to produce $HCOO^-$.[19] It has, however, been reported that $HCOO^-$ formed

† Present address: Institute for Molecular Science, Okazaki National Research Institute, Myodaiji, Okazaki 444, Japan.

(1) Inoue, S., Yamazaki, N., Eds. *The Organic and Bioorganic Chemistry of Carbon Dioxide*; Halstead Press: New York, 1982. Friedli, H.; Lötscher, H.; Siegenthaler, U.; Stauffer, B. *Nature* **1986**, *324*, 237.
(2) Amatore, C.; Savéant, J.-M. *J. Am. Chem. Soc.* **1981**, *103*, 5021.
(3) (a) Ishida, H.; Tanaka, K.; Tanaka, T. *Organometallics* **1987**, *6*, 181. (b) Ishida, H.; Tanaka, K.; Tanaka, T. *Chem. Lett.* **1985**, 405.
(4) (a) DuBois, D. L.; Miedaner, A. *J. Am. Chem. Soc.* **1987**, *109*, 113. (b) Beley, M.; Collin, J.-P.; Ruppert, R.; Sauvage, J.-P. *J. Am. Chem. Soc.* **1986**, *108*, 7461. (c) Pearce, D. J.; Plether, D. *J. Electroanal. Chem. Interfacial Electrochem.* **1986**, *197*, 317. (d) Sullivan, B. P.; Bolinger, C. M.; Conrad, D.; Vining, W. J.; Meyer, T. J. *J. Chem. Soc., Chem. Commun.* **1985**, 1414. (e) Bolinger, C. M.; Sullivan, B. P.; Conrad, D.; Gilbert, J. A.; Story, N.; Meyer, T. J. *J. Chem. Soc., Chem. Commun.* **1985**, 796. (f) Lieber, C. M.; Lewis, N. S. *J. Am. Chem. Soc.* **1984**, *106*, 5033. (g) Hawecker, J.; Lehn, J.-M.; Ziessel, R. *J. Chem. Soc., Chem. Commun.* **1984**, 328. (h) Beley, M.; Collin, J.-P.; Ruppert, R.; Sauvage, J.-P. *J. Chem. Soc., Chem. Commun.* **1984**, 1315. (i) Fisher, B.; Eisenberg, R. *J. Am. Chem. Soc.* **1980**, *102*, 7361.
(5) Ishida, H.; Tanaka, H.; Tanaka, K.; Tanaka, T. *J. Chem. Soc., Chem. Commun.* **1987**, 131.
(6) (a) Nakazawa, M.; Mizobe, Y.; Matsumoto, Y.; Uchida, Y.; Tezuka, M.; Hidai, M. *Bull. Chem. Soc. Jpn.* **1986**, *59*, 809. (b) Slater, S.; Wagenknecht, J. H. *J. Am. Chem. Soc.* **1984**, *106*, 5367. (c) Stalder, C. J.; Chao, S.; Wrighton, M. S. *J. Am. Chem. Soc.* **1984**, *106*, 3673. (d) Kapusta, S.; Hackerman, N. *J. Electrochem. Soc.* **1984**, *131*, 1511. (e) Takahashi, K.; Hiratsuka, K.; Sasaki, H.; Toshima, S. *Chem. Lett.* **1979**, 305.
(7) Ogura, K.; Takamagari, K. *J. Chem. Soc., Dalton Trans.* **1986**, 1519.
(8) Ishida, H.; Tanaka, H.; Tanaka, K.; Tanaka, T. *Chem. Lett.* **1987**, 597.
(9) (a) Becker, J. Y.; Vainas, B.; Eger, R.; Kaufman, L. *J. Chem. Soc., Chem. Commun.* **1985**, 1471. (b) Tezuka, M.; Yajima, T.; Tsuchiya, A.; Matsumoto, Y.; Uchida, Y.; Hidai, M. *J. Am. Chem. Soc.* **1982**, *104*, 6834.
(10) (a) Hiratsuka, K.; Takahashi, K.; Sasaki, H.; Toshima, S. *Chem. Lett.* **1977**, 1137. (b) Meshitsuka, S.; Ichikawa, M.; Tamaru, K. *J. Chem. Soc., Chem. Commun.* **1974**, 158.
(11) (a) Frese, K. W., Jr.; Canfield, D. *J. Electrochem. Soc.* **1984**, *131*, 2518. (b) Canfield, D.; Frese, K. W., Jr. *J. Electrochem. Soc.* **1983**, *130*, 1772.
(12) Frese, K. W., Jr.; Leach, S. *J. Electrochem. Soc.* **1985**, *132*, 259.
(13) Hori, Y.; Kikuchi, K.; Murata, A.; Suzuki, S. *Chem. Lett.* **1986**, 897.

0020-1669/90/1329-0905$02.50/0